

Investigation and modeling of respiratory effects on SCG-signal fiducial points

Rolf Oberlin Hansen

June 6, 2019

Aalborg University



AALBORG UNIVERSITY
STUDENT REPORT

School of Medicine and Health
Biomedical Engineering and Informatics
19gr10405

Master thesis

Investigation and modeling of respiratory effects on SCG-signal fiducial points

Rolf Oberlin Hansen

Supervisor Samuel Emil Schmidt

June 6, 2019

Rolf Oberlin Hansen

Investigation and modeling of respiratory effects on SCG-signal fiducial points

Master thesis, June 6, 2019

Group: 19gr10405

Supervisor: Samuel Emil Schmidt

Aalborg University

Biomedical Engineering and Informatics

School of Medicine and Health

Frederik Bajers vej 7

9220 and Aalborg

Abstract

Different measurement techniques exist for recording cardiac events and diagnosing mechanical heart diseases. These techniques are though often costly, and seismocardiography is a rediscovered and cheaper alternative. The seismocardiography signal is however not fully understood to this day, and part of the reason is that no common morphology has been agreed upon. Parts of this problem is that respiration changes the cardiac event timings and the hearts stroke volume changes up to 30%. Thereto have different interpretations respiration been used. These presentations of respiration have all been segmented and classified into two categories, but in this study is a non-discrete continuous presentation suggested. It is then proposed to create a model for seismocardiography fiducial point amplitudes and timings with respiration phase as an input for the first heart sound, to attempt modelling the morphology. Respiration is successfully derived from the seismocardiography signal and the respiration phase is modeled as a peak-to-peak sine wave, containing information on both respiration amplitude and gradient. Using second degree polynomial regression to fit the fiducial point amplitudes resulted in low and negligible adjusted r^2 values for all 10 study subjects, due to high variance. Tendencies for both amplitude and timings between fiducial points were however discovered, although at different phases. This suggests that a phase delay between respiration and the recorded seismocardiography was evident. The sine wave representation of respiration is recommended for future use in research, since it is evident that non-discrete classification is not suitable for mapping the seismocardiography morphology.

Acknowledgement

I would like to thank my supervisor Samuel Emil Schmidt for excellent supervision and sparring throughout both this project and previous projects. I would thereto like to thank Kim Munck for his voluntary feedback and engagement in this study. Lastly, I would like to thank all my fellow students who voluntarily helped me get data for this study.

Contents

1	Reading guide	1
2	Introduction	5
3	Problem analysis	7
3.1	Mechanisms changing the heart cycle	7
3.2	SCG-morphology	7
3.3	Respiratory classification	9
4	Data	11
4.1	Data recording	11
4.2	ECG	11
4.3	SCG	12
5	SCG derived respiration	15
5.1	Respiration data transformation	16
6	Respiratory effects on fiducial points	19
6.1	Respiratory time-interval changes	24
7	Synthesis	27
	Bibliography	29
A	All polynomial fits	31

Reading guide

Citations in this study follows the Numeric Style, for reference to literature. Abbreviations used in this report are written in full the first time that they are used, followed by their abbreviation in parentheses. The abbreviations are used afterwards and can be found in the Glossary. Each reference to a figure is written as Fig. and each reference to a table is written as Tab. Citations, references and abbreviations are all hyperlinks when viewing the PDF digitally.

Glossary

AC Aortic Closure. 7

AO Aortic Opening. 7, 12, 20, 21, 23, 24, 25

AS Atrial Systole. 7

ECG Electrocardiography. 5, 7, 11, 12

EVF Early Ventricular Filling. 7

IM Isovolumic Moment. 7, 12, 19, 20, 24, 25

MC Mitral Closure. 7, 12, 24, 25

MO Mitral Opening. 7

PAI Peak Atrial Inflow. 7

PSI Peak Systolic Inflow. 7, 12, 24, 25

S1 First heartsound. 7, 8, 20, 27

S2 Second heartsound. 7, 8, 27

SCG Seismocardiography. 5, 7, 8, 9, 11, 12, 15, 16, 19, 22, 23, 24, 27, 28

SVM Support vector machine. 5

Introduction

Seismocardiography (SCG) is a promising technology for measuring vibrations on the chest wall originating in the heart. SCG contains of mechanical events in the cardiac cycle and can be used in conjunction with Electrocardiography (ECG) to provide a detailed description of the hearts condition. Measuring SCG is most commonly performed using an accelerometer attached to the xiphoid process, but can also be obtained using i.e. Doppler ultrasound [6]. Many researchers have suggested that SCG can be utilized in the diagnosing of atrial fibrillation and other heart defects not visible in the ECG-signals. Before effective diagnosing can be accomplished, is it necessary to fully understand the morphology of the SCG-signal. A study by Sørensen et al. [5] mapped the events and fiducial points of the SCG-signal using echocardiography and ECG. The study showed some variation in the timings and morphology in the SCG-signal and other studies have suggested that these changes in the SCG morphology could be caused by respiration [7, 9]. Breathing causes the lungs to inflate or deflate, changing the pressure in the thoracic cavity and on the heart, which changes the pressure gradients on the heart valves [4]. It could therefore be assumed that the cardiac output pr. beat would be lower when expired. To retain a stable cardiac output would it therefore be necessary that the pulse would increase during expired periods in contrast to inspired periods. Pulse should therefore increase during expired periods and that the timings between cardiac fiducial points would be shorter than when inspired [2]. A study by Zakeri et al. [9] regarding detection of respiratory phases, found that timings between fiducial points in the SCG-signal was the best feature to identify respiratory phases using Support vector machine (SVM) with binary classification. Studies regarding SCG-signals all agree that respiration is affecting the mechanical components of the heart, and that both amplitude and timings are affected. It has been shown that the morphology of the SCG-signal changes between the inspiration phase and the expiration phase [4, 3, 9, 8]. No present studies have been made to map the changes of each fiducial point to the corresponding respiration, and thereby the morphological changes of the SCG-signal. Mapping these changes would be beneficial if SCG is to be used as a diagnostic tool, since it would be necessary to know if morphological changes in the SCG-signal are caused by respiration or a disease.

Problem analysis

3.1 Mechanisms changing the heart cycle

The stroke volume of the heart is regulated by the intrinsic mechanisms in the heart, depending almost entirely on the venous return to the heart. Thereto is the heart rate and beat strength also regulated by the autonomic nervous system. The Frank-Starling mechanism of the heart also results in more powerful contractions of the heart when venous return is higher, and weaker contractions are a result of a lower venous return. A higher venous return results in the heart muscles stretching, which enables a more forceful contraction because of the overlap of myosin and actin in the muscles. This Frank-Starling mechanism will therefore adjust the power of the heart contractions in proportion to the venous return.[2] Heart rate changes as an effect of respiration and up to 30% in each respiratory cycle during deep respiration[2]. Since oxygen levels in both blood and lungs are lowered during exhalation is a higher heart rate required to retain sufficient oxygen transportation. Since a more negative pleural pressure increases filling of the right atrium, is the heart rate decreased during inspiration and filling of the lungs. Respiration is therefore changing the heart rate, the beat-to-beat timing and the within beat frequencies[3]. When expiring, will the pleural pressure become more positive, and the venous return of the heart will be lowered. This results in an increased heart rate and reduced contractility during expiration compared to inspiration.

3.2 SCG-morphology

The SCG-signal is comprised of multiple cardiac events often described as fiducial points. These have direct correspondence to the heart cycle given by the ECG-signal and echocardiography images. This was proven by Sørensen et al. [5] who confirmed the labeling of fiducial points in the SCG-signal. Many previous studies regarding SCG have mentioned the lack of a standard interpretation of the events of the SCG-signal, and the study by Sørensen et al. [5] is therefore essential for the research in SCG to progress. The fiducial points annotated in their paper is: Atrial Systole (AS), Peak Atrial Inflow (PAI), Mitral Closure (MC), Aortic Opening

(AO), Peak Systolic Inflow (PSI), Aortic Closure (AC), Mitral Opening (MO) and Early Ventricular Filling (EVF). Some studies also use the Isovolumic Moment (IM) as a fiducial point. The annotations of these points can be found in Fig. 3.1, except for IM, which is located at the valley between MC and AO. The study showed low deviation in the timings of fiducial points within First heartsound (S1) but larger deviations of the fiducial points within Second heartsound (S2). This larger variation in S2 could be because the events within it are harder to detect since they are less distinct than in S1. Variations in timings could be due to random events but could also be due to respiration, since it affects the heart cycle width and timings. Five consecutive SCG cardiac cycles can be seen in Fig 3.2, which shows the respiration affecting their amplitudes a widths.

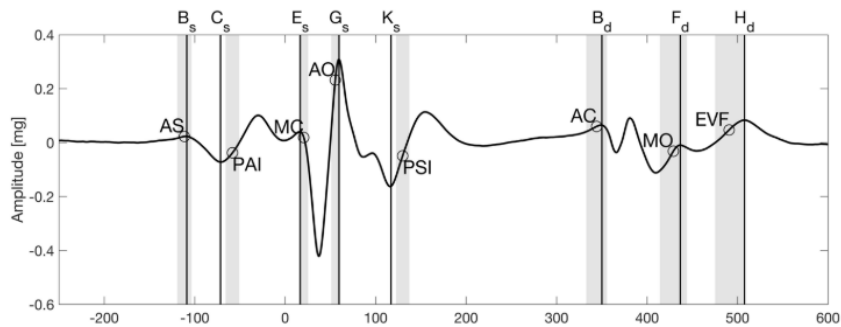


Fig. 3.1.: An SCG-signal with annotations made by Sørensen et al. [5]. These annotations marks S1 and S2 with larger visible deviations(confidence interval = 95%) in S2. The image is created using average heart cycles from multiple subjects. Source: Creative Commons License 4.0 (Definition of Fiducial Points in the Normal Seismocardiogram, Kasper Sørensen, Samuel E. Schmidt, Ask S. Jensen, Peter Søgaaard & Johannes J. Struijk, <https://www.nature.com/articles/s41598-018-33675-6>)[5].

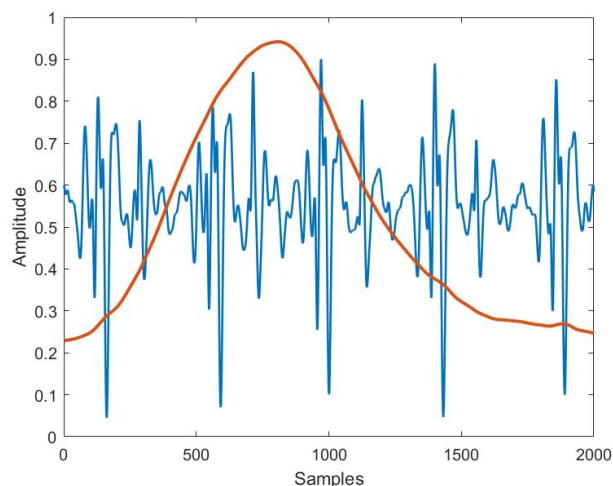


Fig. 3.2.: The figure shows five consecutive cardiac cycles measured with SCG (blue) and the SCG-derived respiration (red) from subject 6. SCG-derived respiration is elaborated in Section 5. The peak of the respiration signal is inhaled, and the bottom is exhaled, showcasing an entire respiratory cycle.

3.3 Respiratory classification

Different papers have attempted to classify heart cycles of SCG-signals in categories of respiration Pandia et al. [3] and Amit et al. [1]. Within these papers have different categories have been used which which are presented in Fig. 3.3. These categories all assumes either that the pressure or pressure change and current pressure of the lungs affects the cardiac cycle equally within these categories. A challenging is task is to create these categories since heart cycles on the fringe of two categories are very similar and therefore difficult to classify. Thereto, using only two or four categories for classification reduces the amount of information regarding the cardiac cycles and their corresponding respiration, due to generalization within the categories. Studies have also showed that both the relative pressure in the chest cavity and the pressure gradients change the morphology of the SCG-signal. Categories including both inspirating and expiring phases will therefore be even more difficult to classify.

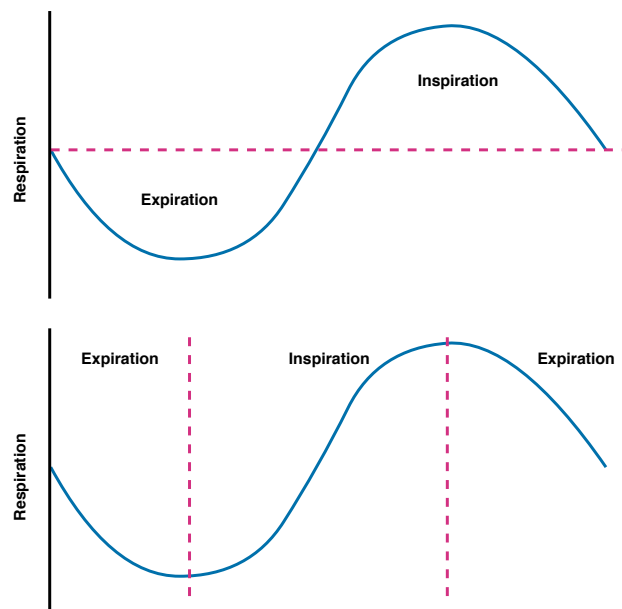


Fig. 3.3.: Two different approaches used to separate respiration which are commonly used in SCG studies Pandia et al. [3] and Amit et al. [1]. Respiration is separated as pressure in the top graph and separated by pressure gradient in the bottom graph.

Since categorization of respiration has proven difficult could a possible solution to understand the effect of respiration on the SCG-signal, be to treat the changes in morphology for each fiducial point within the signal as a function of pressure and pressure change. This would allow for estimates of the SCG-signal to every possible state of normal respiration.

The aim of this study is to map the changes of the fiducial points of the SCG-signal to respiration, without using classification.

Data

4.1 Data recording

Two-lead ECG-, respiration- and SCG-signals were recorded from 10 healthy males age 25.3 (24-28) from Aalborg university, Denmark and University of Turku, Finland. ECG was recorded as an indicator for beginning of cardiac cycles and a reference for fiducial point annotations in the SCG-signals. Of these 10 subjects, were 7 recorded by the author, at Aalborg university, for this project specifically. Respiration was recorded using a strain gauge belt attached to the subjects abdomen. SCG was recorded in the z-axis on the subjects xiphoid process using an ADXL355 accelerometer. This was only done for 7 of the 10 subjects. The SCG-signals were recorded using a single accelerometer placed on the xiphoid process. All recorded signals were sampled at 500 Hz in LabView, which was deemed sufficient since the SCG-signal's highest frequency is at 90 Hz following the filtering of Sørensen et al. [5]. Each subject was recorded for three minutes lying horizontally and breathing in a rhythm that felt normal to each individual subject. Before filtering and detection of fiducial points in the signals, was a manual selection of usable periods of measurement performed. Discarded periods of measurement included: coughing, detached measurement equipment, unidentifiable events in the cardiac cycle and non-heart related movement.

4.2 ECG

The ECG-signal was filtered using a 4th order zero-phase digital Butterworth band-pass filter (1-80 Hz) and afterwards multiplied exponentially to successfully detect the r-peak. This process made it easier to distinguish between the r-peak and the t-wave of the ECG-signal. All r-peaks of the ECG-signals were then automatically labeled using a threshold and the findpeaks function of MATLAB.

4.3 SCG

The z-axis SCG-signal was filtered with a 1st order zero-phase digital Butterworth highpass filter (0.01 Hz) to remove dc components and offset, and afterwards filtered with a 3rd order zero-phase digital Butterworth lowpass filter (90 Hz) to remove non-SCG relevant components. SCG-signals were then normalized in amplitude for each subject, so that the highest recorded amplitude was 1 and the lowest recorded amplitude was set to 0.

Amplitude for each fiducial point was found using search windows based on the timing of the r-peak in the ECG-signal. A threshold was created to find the r-peak and from it the AO-peak of the SCG-signal which occurs short after. The AO-peak location was then used to localize the local minimums of IM and PSI. The MC fiducial point was then found as a peak prior to the location of the IM fiducial point. An illustration showing the search windows can be seen in Fig. 4.1. The search windows used for automatically detecting fiducial points were adjusted for each subject. Each found fiducial point was afterwards corrected using the criteria:

- Is there a corresponding ECG cardiac cycle, if not - discard the cardiac cycle.
- Are the fiducial points correctly placed, if not - manually correct them if possible.
 - Is it possible to manually identify the fiducial points, if not - discard the cardiac cycle.
 - Is the cardiac cycle unaffected by external noise, if not - discard the cardiac cycle.

Not all subjects had a distinct MC fiducial point, which meant that no MC fiducial point was annotated for these three subjects. Amplitude of each fiducial point and the number of samples between them and the AO fiducial point was saved for each cardiac cycle. The number of cardiac cycles and fiducial points for each subject, as well as used filters can be found in Tab. 4.1.

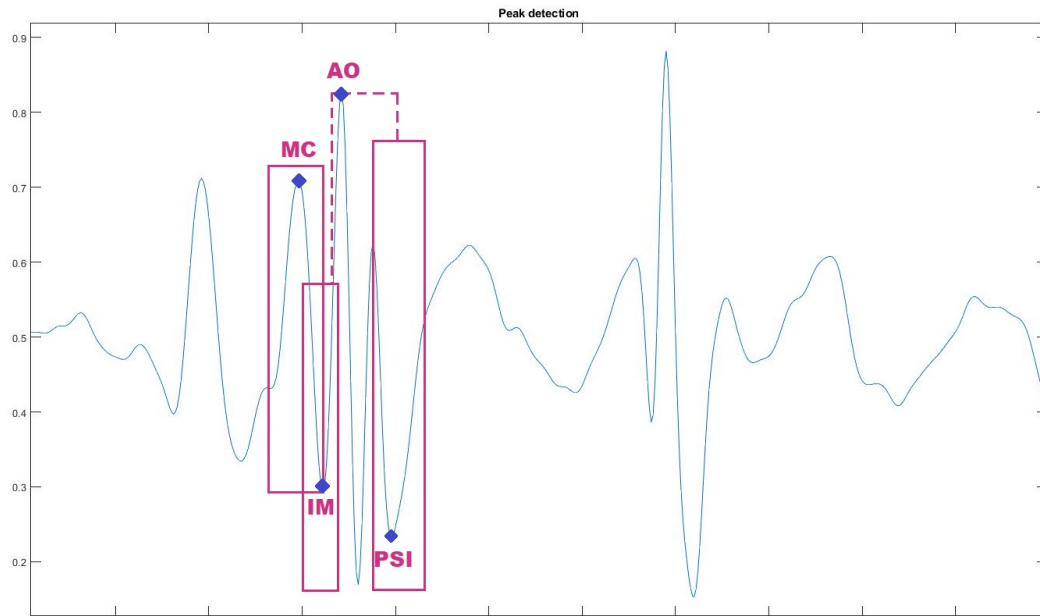


Fig. 4.1.: The figure illustrates the labeling of SCG fiducial points of subject 8, based on the location of the AO peak. From it are the minimums of IM and PSI found, and from IM is MC found as a maximum.

ID	Age (Years)	Height (cm)	Weight (kg)	HR (bpm)	MC (n)	IM (n)	AO (n)	PSI (n)
1	24	194	100	61.9	137	131	136	123
2	24	184	63	51.6	89	91	95	93
3	25	185	80	78.8	62	81	81	78
4	24	174	72	87.7	NONE	64	65	65
5	28	185	85	83	103	242	249	235
6	26	183	81	85.3	NONE	105	105	103
7	25	181	73	54.2	128	130	138	130
8	24	168	80	75.6	220	223	222	211
9	24	182	65	79.8	288	288	292	264
10	26	172	70	66.4	NONE	117	118	107

Tab. 4.1.: Data for each subject included in this study. Height is in cm, weight is in kg and heart rate (HR) is in bpm. Lastly are the number of annotated fiducial points pr. subject presented

SCG derived respiration

In order to investigate how respiration affects the SCG-signal, is it necessary to have a comparable respiration measurement between the subjects. Deriving a respiration signal from the recorded accelerometer data measuring SCG will provide a respiration signal recorded at the xiphoid process for all subjects. It is essential to interpret the differences between a measured respiration-signal and a respiration signal derived from an SCG-signal, to validate if the measured respiration signal can be substituted. Since there is a delay between the measuring at the abdomen and at the xiphoid process, was it investigated how much the abdominal respiration-signal should be shifted to maximize correlation between the two respiration signals. Thereto, two subjects were missing measured respiration, which could be substituted using SCG derived respiration. The measured respiration signals were filtered using a moving average filter with a window size of 50 samples to remove the high frequency noise. Since breathing patterns vary between subjects, are different zero-phase Butterworth filters used to derive the respiration from the raw unfiltered SCG-signal. Filter coefficients and number of respiratory cycles signals for each subject can be seen in Tab. 5.1.

ID	Respiratory cycles	Low-pass	High-pass
1	49	1hz 2.Ord	0.1hz 2.Ord
2	69	0.3hz 2.Ord	0.3hz 4.Ord
3	22	0.2hz 2.Ord	NONE
4	17	0.2hz 2.Ord	NONE
5	93	0.2hz 2.Ord	NONE
6	32	0.2hz 3.Ord	NONE
7	69	0.2hz 4.Ord	NONE
8	57	0.2hz 3.Ord	NONE
9	46	0.2hz 7.Ord	NONE
10	29	0.2hz 3.Ord	NONE

Tab. 5.1.: The number of respiratory cycles included for each subject in the study, followed by the filter cutoff frequencies and orders used to extract them. All used filters are zero-phase Butterworth filters.

Both SCG derived- and measured respiration signals were normalized as the same way as the SCG-signal as described in 4.3. This process of normalization made the SCG derived- and measured respiration comparable with regards to amplitude. A comparison of these two respiration signals was then made for each subject in order to validate whether SCG derived respiration could be used as respiration. Fig. 5.1

shows the recorded respiration signal compared to the SCG derived respiration signal. It is to be expected that the amplitudes and timings between the compared signals vary, since they are recorded at different places (abdomen and xiphoid process). The form is similar and the number of peaks identical. It is therefore decided that using SCG derived respiration will yield a more accurate representation of the respiration's effect on the heart.

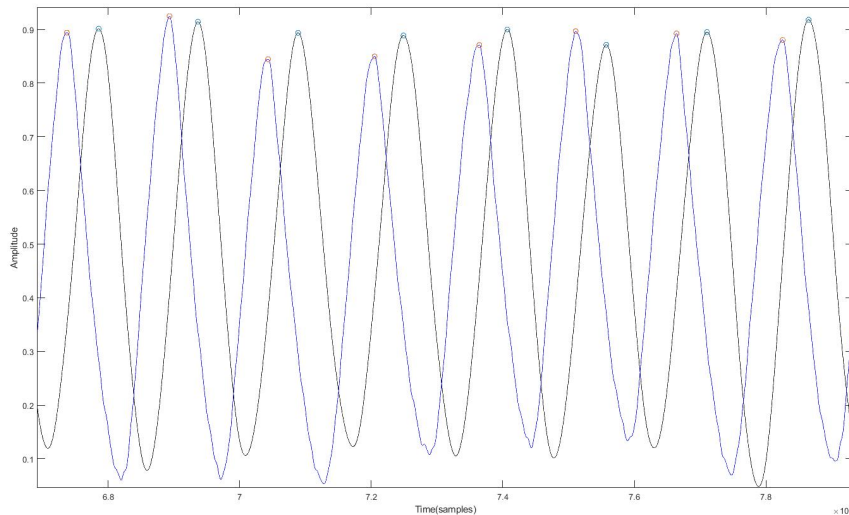


Fig. 5.1.: SCG derived respiration (black) compared with measured respiration (blue) from subject 6. Registered peaks when inhaled are marked with an 'o'.

5.1 Respiration data transformation

Previous attempts regarding utilization of respiration have used categorization of respiration, whereas a non-discrete variable could be more informative, as elaborated in Section 3. In an effort to create a continuous non-discrete variable has respiration been transformed into sinusoidal functions. Each respiration cycle, inhaled to exhaled to inhaled, has been modelled as a first order sinusoidal function using MATLAB's Curve Fitting function. The argument for creating multiple sinusoidal functions is that the frequency of the respiration cycles reduces over the span of the data recordings for each subject. Using sinusoidal functions enables the usage of π and radians to describe the phase of the respiration cycle, which contains information on both amplitude and phase of the respiration. An illustration showing the fitted sinusoidal function to a respiratory cycle can be seen in Fig. 5.2. Separating each respiratory cycle into individual sinusoidal functions does also works as a way to normalize respiration. This is not a problem since all subjects where instructed to breathe normally, resulting in similar amplitudes, but could pose a problem if to many variations occurred during data collection.

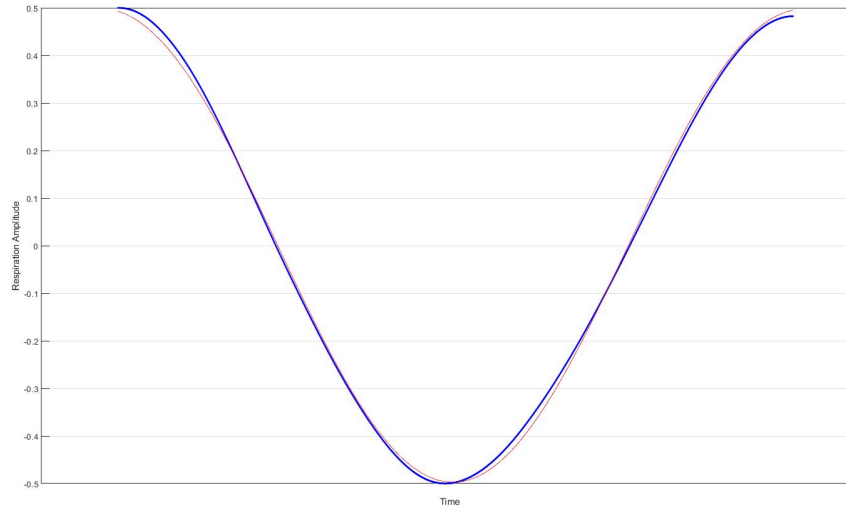


Fig. 5.2.: A single respiratory cycle from subject 5. The actual respiration cycle from peak inhale to peak inhale presented as the blue curve. The fitted first order sinusoidal function presented as the red curve, from -0.5π to 1.5π .

The output of the data transformation from time vs. amplitude to phase vs. amplitude, results in every respiratory cycle being expressed as an amplitude and a phase between 0.5 and 2.5π . Since the sine of 0 is 0 and the sine of 2π is also 0 , will both correspond to mid-inhale. π will therefore correspond to mid-exhalation and 0.5π and 1.5π corresponds to peak inhaled and peak exhaled respectively. π allows for creating an ellipse function describing fiducial point amplitude with regards to the respiratory phase. This concept is shown in Fig. 5.3.

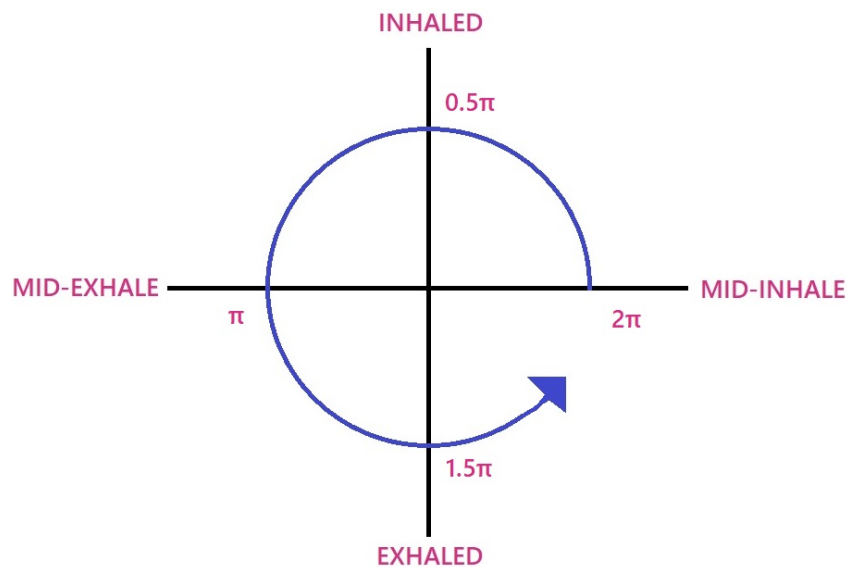


Fig. 5.3.: Explanation of the sine phase of the respiration compared to the π value.

Respiratory effects on fiducial points

The interaction between respiration and SCG fiducial points have been transformed into a cyclical form. This chapter presents the respiratory effects on SCG fiducial point amplitudes and timings. An elliptical fit using a least squares fit, was created for each subject, based on SCG fiducial point amplitudes and respiratory phase. Such an elliptical fit and the corresponding data points can be seen in Fig. 6.1. For clarity is the same data as a plotted as π vs. fiducial point amplitude with a second order polynomial fit in Fig. 6.2. Elliptical fit is used instead of circular fit, since the objective of this study is to investigate changes in fiducial point amplitude and timings, suggesting that this change is evident. The fiducial point amplitudes are transformed into a circular form using the following equations for the coordinates:

$$xcoord = y * \cos(x)$$

$$ycoord = y * \sin(x)$$

In the equations is y the amplitude of the fiducial point, and x is the phase of the respiratory cycle of the fiducial point ($0-2\pi$). These trigonometric equations creates a circular scatter of samples where the radius from origo is the fiducial point amplitude, and the angle from $(x,y) = (R_{\neq 0}, 0)$. An elliptical fit can then be created using the least squares method, resulting in the following formula for the ellipse:

$$\frac{((x - h)\cos(A) + (y - k)\sin(A))^2}{(a^2)} + \frac{((x - h)\sin(A) - (y - k)\cos(A))^2}{b^2} = 1$$

In the equation is h and k the center shift and a and b are tilt. A is the angle measured from the x-axis. Finally is a second order polynomial used with the equation:

$$f(x) = ax^2 + bx + c$$

In the equation is a the exponential increase or decrease, b defines the peak of the curve and c defining the offset..

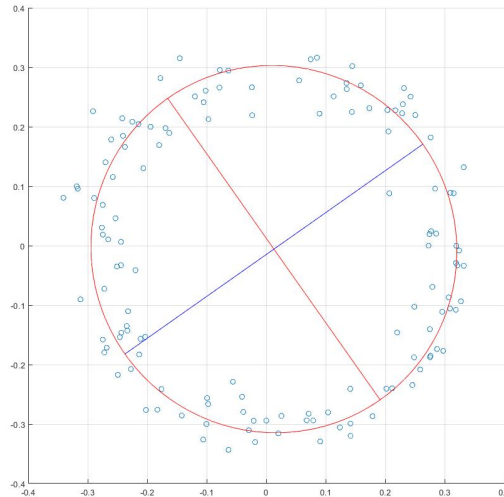


Fig. 6.1.: An elliptic fit for the IM fiducial point for subject 6. The amplitude of the fiducial points is the euclidean distance from the center to the circle or data point. The ellipse follows π with one counter-clockwise revolution equal to one respiratory cycle, starting in $y = 0$ and x being positive. The blue line indicates the short axis of the ellipse and the red line indicates the long axis of the ellipse.

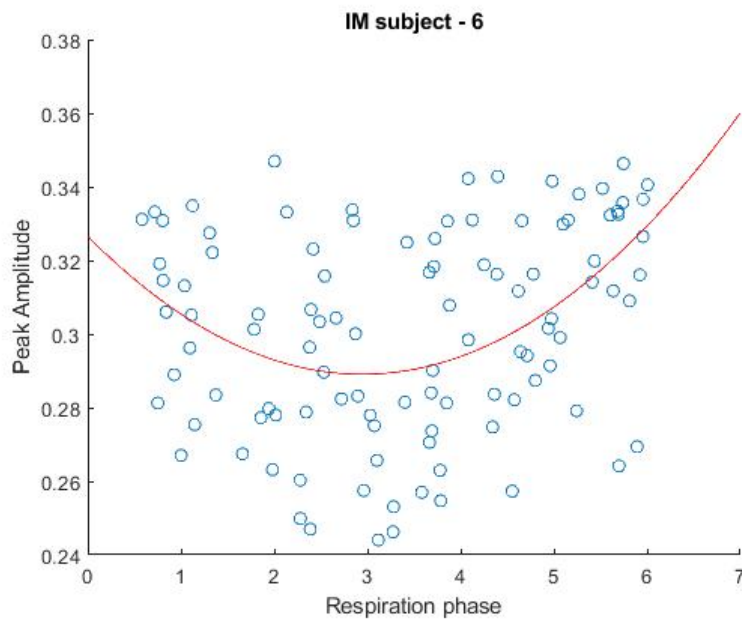


Fig. 6.2.: A second order polynomial fit for the IM fiducial point for subject 6. The data points are fiducial point amplitudes and their corresponding π value (0-2 π) obtained from the sinusoidal fit elaborated in section 5.1. $r^2 = 0.09346$ and $p = 0.05810$

Fig. 6.1 shows that the center of the ellipse is located at origo, but with x being slightly positive. This suggest that the overall amplitude of the IM peak is lower at 0.5 to 1.5 π , meaning that the amplitude is reduced between the exhaling period,

compared to the inhaling period. This is also evident when investigating Fig. 6.2, which shows the same tendency. However, the ellipse does appear almost circular, which means that almost no change in amplitude is caused by pleural pressure change during inhaling and exhaling. This could be because all the points used creating the elliptical fit are assumed to have the same timing. Since both timing and amplitude change of the fiducial points are correlated with respiration change, could it also be assumed that amplitude change and timing of the fiducial points are correlated. Testing for this correlation gives $r = -0.1206$ and $p = 0.1667$, indicating a less than significant correlation. The test indicates that an increase in amplitude fiducial point for IM results in a decrease in timing between AO and IM. This correlation means that decreased heart rate correlates with decreased stroke volume, identical to the physiology described in Section 3. The p-value is however high, indicating a insignificant correlation. To prove the amplitude of S1 is shortened during S1 for this subject, is the first order sinusoidal fit for AO respiration vs. amplitude created in Fig. 6.3. The figure shows an increase in amplitude of AO at around 1π , which is when the subject is fully inhaled. This increase in amplitude combined with the decrease in amplitude for IM when inhaled, supports the physiology, described in Section 3, of a shortened S1 amplitude and timing when exhaled. The r^2 is however very low for both of the fits in both Fig.6.2 and 6.3, indicating that the within subject variability is high.

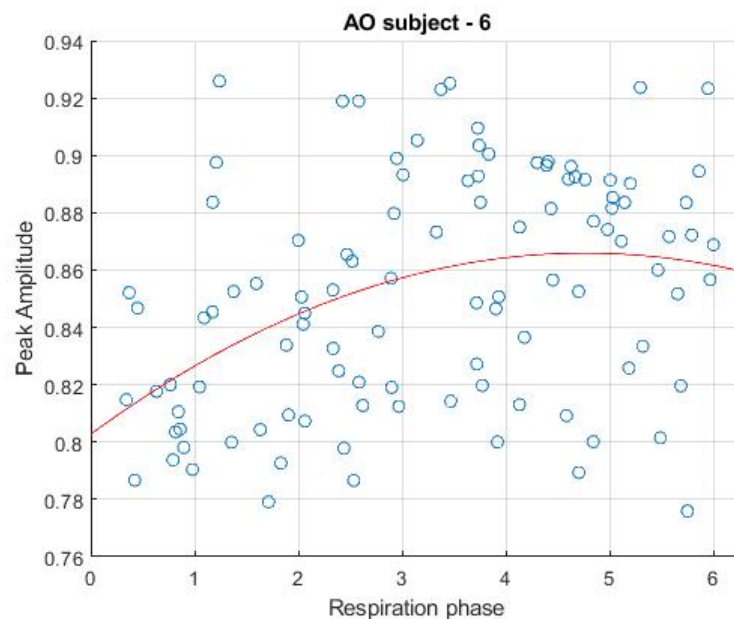


Fig. 6.3.: A polynomial fit for the AO fiducial point for subject 6. The data points are fiducial point amplitudes and their corresponding π value ($0-2\pi$) obtained from the sinusoidal fit elaborated in section 5.1. $r^2 = 0.15561$ and $p = 0.00018$

The second order polynomial fit for each fiducial point amplitude can be seen in Fig. 6.4 Goodness-of-fit measures for each fiducial point regression for each subject can

be found in Tab 6.1, using r^2 for fit and p for determining significance. All polynomial fits for each individual subjects with data points can be found in Appendix A.

ID	MC		IM		AO		PSI	
	r^2	p	r^2	p	r^2	p	r^2	p
1	0.07944	0.11625	0.00529	0.88509	0.01705	0.31867	0.04651	0.0574
2	0.05331	0.25424	0.01738	0.64517	0.28712	0	0.12192	0.00288
3	0.02537	0.62161	0.11322	0.13770	0.31641	0	0.30182	0
4	NONE	NONE	0.40470	0.00724	0.07027	0.10449	0.18053	0.00209
5	0.08983	0.17529	0.07264	0.01044	0.11793	0	0.12643	0
6	NONE	NONE	0.09346	0.05810	0.15561	0.00018	0.00195	0.90693
7	0.04347	0.16899	0.02898	0.39605	0.01562	0.34547	0.07235	0.00849
8	0.11382	0.00138	0.03293	0.14578	0.25954	0	0.05647	0.00237
9	0.02181	0.30737	0.05313	0.05244	0.05159	0.00047	0.10817	0
10	NONE	NONE	0.17234	0.00235	0.21622	0	0.37994	0

Tab. 6.1.: r^2 and p-value for all second order polynomial fits for all subjects and their fiducial points. Each value is rounded up with 5 decimals with 0 being less than 0.000005. The goodness-of-fit measures relates to the fits of Fig. 6.4.

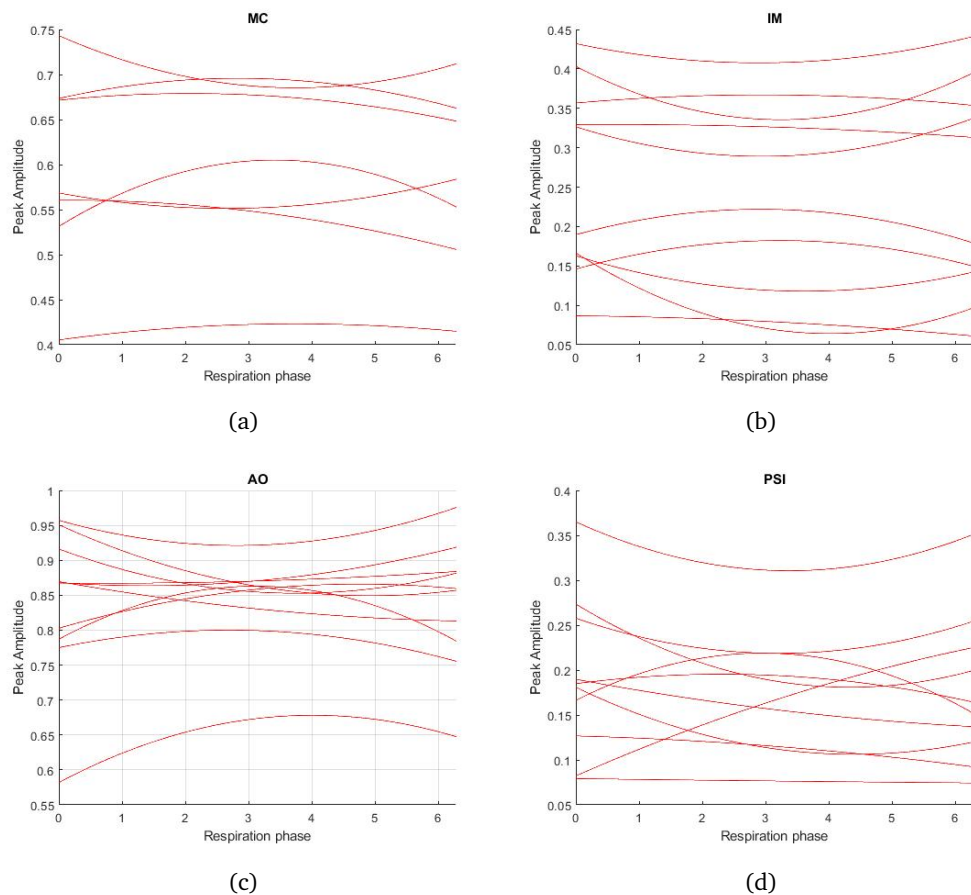


Fig. 6.4.: The second order polynomial regression plots for each fiducial point and each subject showing the tendency of amplitude during the respiratory cycle. SCG-derived respiration is used for all subjects. The x-axis shows the phase of respiration with 0 and 2π being mid-inhale and the y-axis being fiducial point amplitude. (a) Amplitude of MC from 7 subjects; (a) Amplitude of IM from 10 subjects; (b) Amplitude of AO from 10 subjects; and, (c) Amplitude of PSI from 10 subjects.

It is evident when investigating 6.4 that the fiducial points have different tendencies across the subjects. This does not support the physiology described in Section 3, that fiducial points follow a specific behavior. To ensure the inter-subject variability in fiducial point amplitudes is not caused by utilizing SCG derived respiration, was fiducial point amplitude also investigated for measured respiration. Tendency of the fiducial point amplitudes did however also vary between the subjects, when using the measured respiration, as evident in Fig. 6.5.

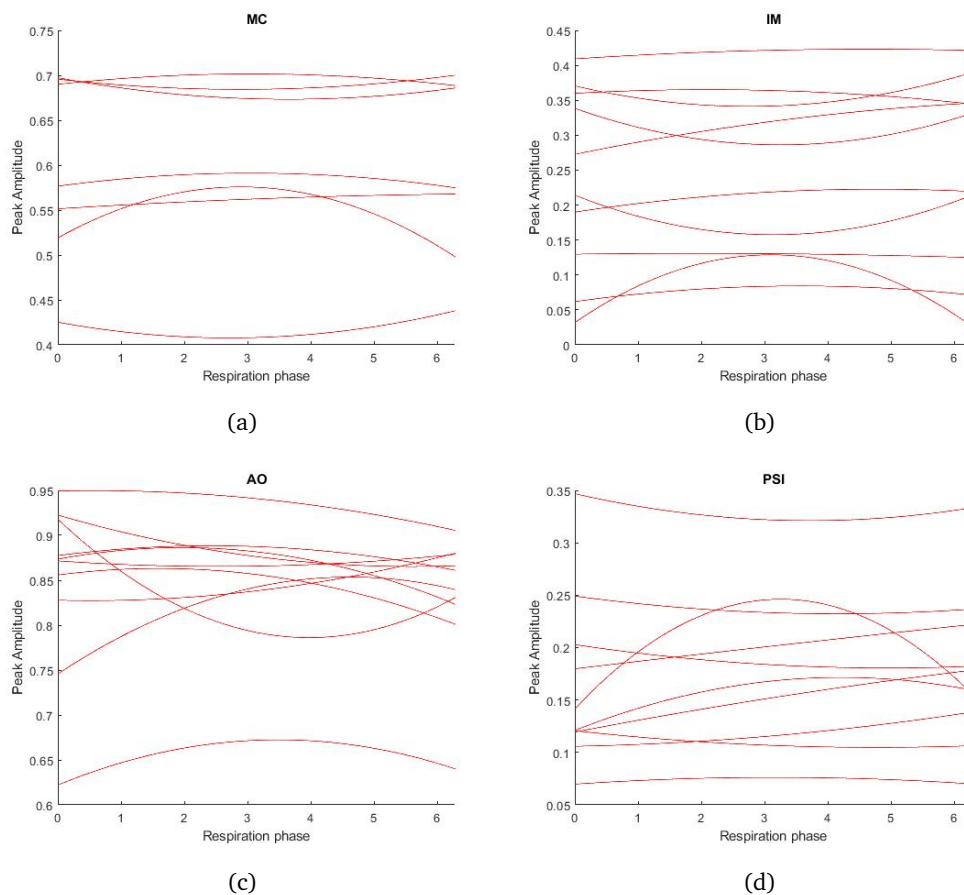


Fig. 6.5.: Second order polynomial regression of fiducial point amplitudes during respiration, using measured respiration instead of SCG-derived respiration. (a) Amplitude of MC from 7 subjects; (b) Amplitude of IM from 10 subjects; (c) Amplitude of AO from 10 subjects; and, (c) Amplitude of PSI from 10 subjects.

Both the types of respiration used to express how the respiration affect the SCG fiducial points have inter-subject variability. It is therefore investigated if the tendencies of fiducial point amplitudes are similar across the subjects when all points are grouped by timings. 50% of the samples with shortest timing between AO and the other fiducial points were grouped and had a second order polynomial regression performed. This gave an inter-subject variability similar to those presented in Fig. 6.4 and Fig. 6.5, as seen in Fig. 6.6 containing the grouped samples. It is therefore

decided to investigate in any tendencies between respiration and timings exists, excluding fiducial point amplitudes.

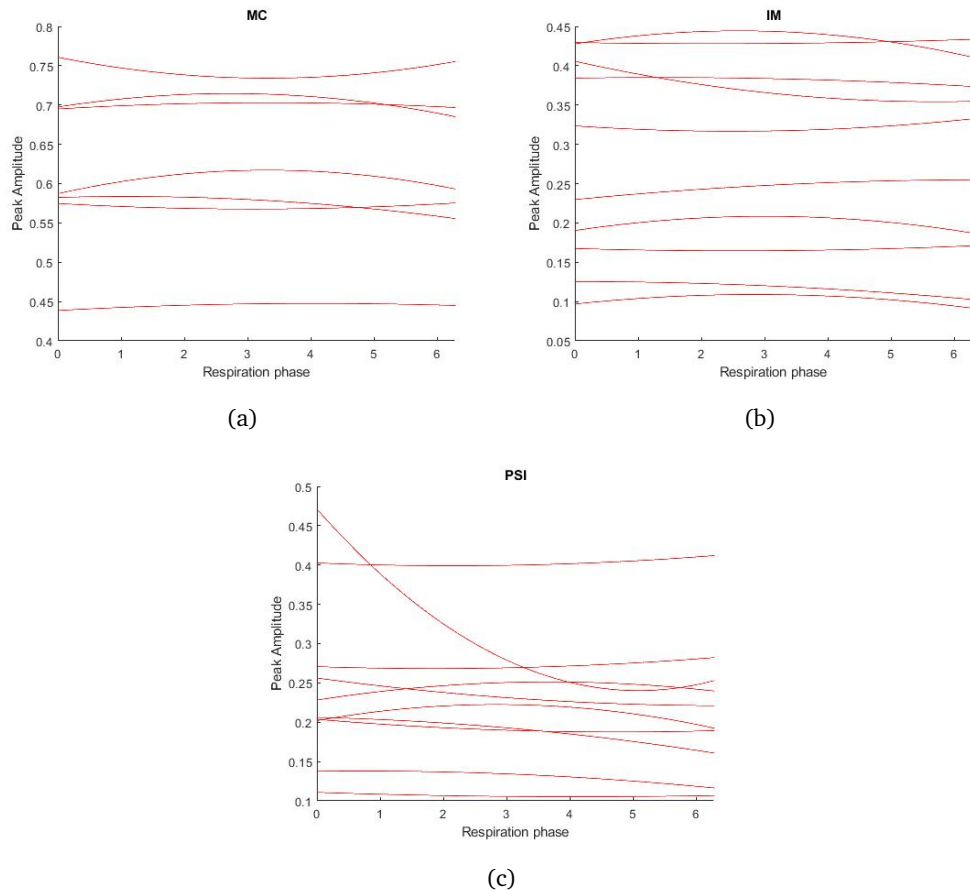


Fig. 6.6.: Amplitude of fiducial points during respiration. Only 50 % of the are included, which are samples with a shorter timing between AO and the respective fiducial points. (a) Amplitude of MC from 7 subjects; (b) Amplitude of IM from 10 subjects; and, (c) Amplitude of MC from 10 subjects.

6.1 Respiratory time-interval changes

As described in Section 3, are changes in respiration affecting the heart rate, and these effects are investigated in this section. Change in heart rate is measured as the increase or decrease in timings between fiducial points in the SCG-signal. A decrease in samples between fiducial points from same cardiac cycle means a shorter cardiac cycle, thereby an increased heart rate and vice versa. The difference in timings between fiducial points are presented as timing difference between AO fiducial points and the remaining fiducial points of S1. These timings have been normalized due to between subject variability, and therefore made them more comparable. Sampling frequency has also made the timings grouped since the variance in timing for each fiducial point is very low. Changes in timings due to respiration are presented as

heat maps for MC, IM and PSI in Fig. 6.7. The reason for using heatmaps and not regression, is that the sample rate of 500 and the small changes in timings results in bins of data. Regression would only be suitable if a higher sample rate was used, allowing for more detailed information regarding distances between fiducial points.

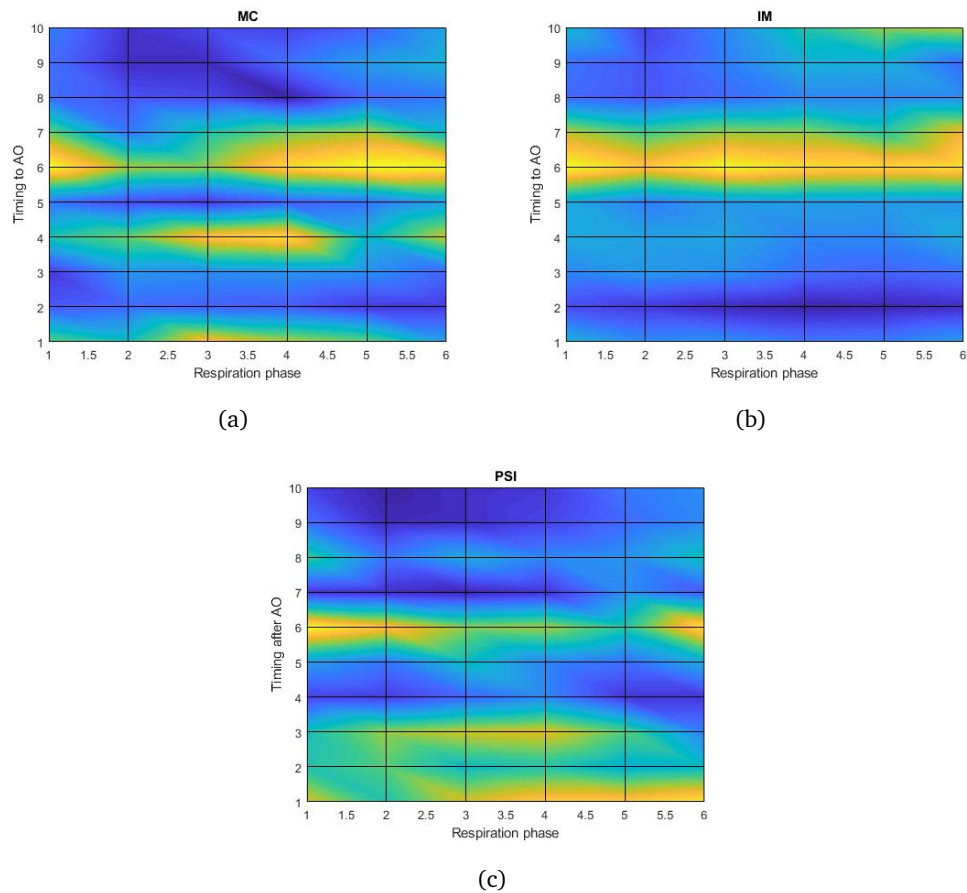


Fig. 6.7.: Heat maps showing the density of samples located at certain timings before and after the AO fiducial point. The intensity in yellow corresponds to high density of samples, and a dark blue corresponds to low density of samples. The y-axis is normalized in distance, with 1 corresponding to the lowest number of samples between AO and the presented fiducial point for each subject. 10 on the y-axis is therefore the corresponding maximum number of samples for each individual subject. The x-axis is the respiration phase separated into 6 bins (a) Timing from MC to AO from 7 subjects; (b) Timing from IM to AO from 10 subjects; and, (c) Timing from AO to PSI from 10 subjects.

The heat maps of Fig. 6.7 reveals a tendency of the MC fiducial point being closer to AO during the expired period. The same tendency exists for PSI, where the fiducial point occurs more closely to AO during expired periods. The heat map for IM in Fig. 6.7(b) does however not reveal any change in timing due to respiration, except increase during full expiration. The heat maps for MC and PSI does thereby support the hypothesis of increased width of S1 during expired phases. This hypothesis is

however not supported by the timing of IM. The heat maps of Fig. 6.7 have many bright yellow spots, which indicates high inter-subject variance in the timing of fiducial points.

Synthesis

An individual model could be created as evident by Section 6 where subject 6 was presented in detail. The z-axis boundaries would be defined as the longest and shortest difference in timing between two fiducial point. The circumference could afterwards be calculated for each timing by utilizing the sine wave representation of the respiration as presented in Section 6. This creates a single input model for describing the changes of the fiducial points in an SCG-signal. The reason for not creating an overall model and testing it between subjects, was that both fiducial point amplitude and timings behaved differently across the subjects. The respiration, both measured and SCG derived, is most likely the cause of this inter-subject difference. This is why the behavior of fiducial points for most subjects were very similar, but at different phases. This is evident when investigating Fig. 6.5, showing all the second order polynomial regression of the fiducial point amplitudes. In the figure are almost all of the regression curves of the same amplitude and curvature across a respiration cycle. Since each regression is created on only a single subject, could a phase difference between the cause inter-subject variance. This was partly the reasoning behind investigating multiple respiration representations, but a common behavior of the fiducial point amplitudes could not be found. SCG derived respiration did have the same shape and amplitude as the measured respiration, and could successfully be derived for all subjects. SCG derived respiration and the transformation of respiration into sine waves could however only be used on respiratory cycle with same peak inhale amplitudes. Thus were all deviating respiratory cycles and their corresponding SCG fiducial points discarded. The polynomial regressions did have high variance and did therefore not a very high r^2 . In the cases where the p -values were low, were the r^2 however higher, indicating that the fit was significant when the correlation was higher. There is similarly a high variance in timing of fiducial points across all subjects. Variance in both amplitude and timings of the fiducial points could be caused by other intrinsic factors or mechanisms regarding the respiration.

It was hypothesized that inhalation and exhalation would have opposite effects on the SCG-signals fiducial points. There could however be differences in how much the different phases of respiration affect the fiducial points, and a more advanced shape could perhaps be more accurate. Such a shape could be a more egg formed circular shape. It would of course first be necessary to verify how the respiration affects the SCG-signal.

One subject did have a much larger S2 than their S1. This resulted in fiducial point amplitudes deviating from the rest after the normalization. This is because the normalization was made based on highest and lowest amplitudes for each subject. The normalization could perhaps have been performed based on highest and lowest S1 fiducial point amplitude, which could have made all the subjects more comparable.

The sample frequencies used for this study did also pose a problem when investigating the timings of the fiducial points. Fiducial points for subjects with a high heart rate had so small differences in timings. This meant that the resolution provided by a 500 Hz sampling rate rounded timings up and down. This resulted in a very discrete signal with bins of data, as evident when investigating Fig. 6.7. If timings between fiducial points should be mapped and modelled detailed, would a higher sample frequency be recommended. Variance is however high for timings of fiducial points, and modelling the exact timing difference may not be necessary from a clinical standpoint, depending on the specific fiducial point.

Even though the tendencies for the fiducial point changes during respiration were differing, was it still discovered that the behavior of these fiducial points were non-discrete. Classification of SCG cardiac cycle have previously struggled in finding a common way of defining the respiratory cycles. It is from this study suggested that a non-discrete representation of respiration is a more accurate tool when defining the SCG morphology, and could possibly be the standard adapted for describing respiratory changes.

Bibliography

- [1]Guy Amit, Khuloud Shukha, Noam Gavriely, and Nathan Intrator. „Respiratory modulation of heart sound morphology“. In: *AJP* 296.3 (2009), H796–H805 (cit. on p. 9).
- [2]Arthur C. Guyton and John E. Hall. *Textbook of Medical Physiology ELEVENTH EDITION*. ELSEVIER SAUNDERS, 2006, pp. 1011–1018 (cit. on pp. 5, 7).
- [3]Keya Pandia, Omer T. Inan, and Gregory T A Kovacs. „A frequency domain analysis of respiratory variations in the seismocardiogram signal“. In: *EMBS 2013* (2013), pp. 6881–6884 (cit. on pp. 5, 7, 9).
- [4]Keya Pandia, Omer T Inan, Gregory T A Kovacs, and Laurent Giovangrandi. „Extracting respiratory information from seismocardiogram signals acquired on the chest using a miniature accelerometer“. In: *Physiological Measurement* 33.10 (2012), pp. 1643–1660 (cit. on p. 5).
- [5]Kasper Sørensen, Samuel E. Schmidt, Ask S. Jensen, Peter Søgaaard, and Johannes J. Struijk. „Definition of Fiducial Points in the Normal Seismocardiogram“. In: *Scientific Reports* 8.1 (2018) (cit. on pp. 5, 7, 8, 11).
- [6]Kouhyar Tavakolian and Andrew P Blaber. „Estimation of hemodynamic parameters from seismocardiogram“. In: *Computing in Cardiology* (2010), pp. 1055–1058 (cit. on p. 5).
- [7]Kouhyar Tavakolian, Ali Vaseghi, and Bozena Kaminska. „Improvement of ballistocardiogram processing by inclusion of respiration information.“ In: *Physiological measurement* 29 (2008), pp. 771–781 (cit. on p. 5).
- [8]Christian Ulrich, Rolf Hansen, Farzad Khosrow-khavar, et al. „Determining the Respiratory State From a Seismocardiographic Signal–A Machine Learning Approach“. In: *2018 Computing in Cardiology Conference (CinC)* 45 (2019), pp. 1–4 (cit. on p. 5).
- [9]Vahid Zakeri, Alireza Akhbardeh, Nasim Alamdari, et al. „Analyzing Seismocardiogram Cycles to Identify the Respiratory Phases“. In: *IEEE* 64.8 (2017), pp. 1786–1792 (cit. on p. 5).

All polynomial fits

